Bull. Mar. Sci & Tech 11(1), 2002
Research Institute of Marine Science and Technology
Korea Maritime University

A finite element method for dynamic analysis of long slender marine structures under combined parametric and forcing excitations

Han-Il Park [a,*], Dong-Ho Jung [b]

[a] *Division of Ocean Development Engineering, Korea Maritime University, Dongsam-dong, Youngdo-ku, Pusan 606-791, South Korea*
[b] *Department of Ocean Development Engineering, Graduate School of Korea Maritime University, Dongsam-dong, Youngdo-ku, Pusan 606-791, South Korea*

Received 28 June 2001; accepted 22 August 2001

Abstract

This paper presents a numerical analysis of lateral responses of a long slender marine structure under combined parametric and forcing excitations. In the development of the 3-D numerical program, a finite element method is implemented in the time domain using the Newmark constant acceleration method. Some example studies are performed for various water depths, environmental conditions and vessel motions. The relative amplitudes of combined excitations to a conventional forcing excitation are examined. The response amplitude of a combined excitation is much greater than that of a forcing excitation in the even number of instability regions of the Mathieu stability chart. The results demonstrate that a combined excitation needs to be considered for the accurate dynamic analysis of long slender marine structures subjected to a surface vessel motion.

Keywords: Slender marine structures; 3-D dynamic analysis; Finite element method; Combined excitation; Dynamic stability

* Corresponding author. Tel.: +82-51-410-4326; fax: +82-51-404-3538.
E-mail address: hipark@kmaritime.ac.kr (H.-I. Park).

1. Introduction

Long slender marine structures such as risers, TLP tethers as shown in Fig. 1 are mostly subjected to two directional sources of dynamic excitations; the first source of dynamic excitation is induced by horizontal forces from platform surge motions and direct wave forces whereas the second source is due to changes in axial tension by heaving motion of a platform. The first and second sources are respectively called as a forcing excitation (or external excitation) and a parametric excitation. When two sources of dynamic excitations are considered simultaneously, that is more realistic, the dynamic behavior of long slender structure becomes a combined forcing and parametric excitation problem.

The forcing excitation problem (a forced vibration problem) has been extensively studied. Patel and Witz (1991) introduces several kinds of forcing excitation problems of TBP tethers and risers. Most research on dynamics of slender marine structures fall in this category (Kirk et al., 1979; Dareing and Huang, 1979; Kim and Triantafyllou, 1984; Kokarakis and Bernitsas, 1987).

A parametric excitation problem is also partly investigated by Hsu (1975), Strickland and Mason (1981), Moe et al. (1987), Ohkusu (1990) and Patel and Park (1991). More recently, a combined excitation problem has been studied. Haquang and Mook (1987) reported the non-linear structure vibrations under combined parametric and external excitations. Thampi and Niedzwecki (1992) examined the response of a non-linear marine riser to combined excitations by using Markov methods. Patel and Park (1995) researched dynamic responses of TLP tethers under combined excitations by a semi-analytical method. Ryu and Isaacson (1998) investigated 2-D dynamic response of slender maritime structure under regular waves and vessel motions that induces a combined excitation.

This paper presents a 3-D dynamic analysis of a long slender marine structure under combined heave and surge motions at the top end to clarify in detail the effects of combined excitations. The analysis is performed in the time domain by using a finite element method. Some example studies are performed for various cases.

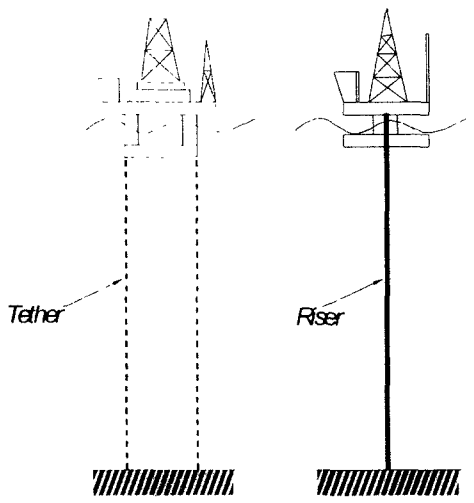

Fig. 1. Some examples of slender marine structures under dynamic excitations.

2. Governing equation

The governing equations of lateral motions of a slender marine structure are written as (see Fig. 2 for notations);

$$\frac{\partial^2}{\partial z^2}\left(EI\frac{\partial^2 y}{\partial z^2}\right)-[T(z)-S\cos\omega t + A_oP_o-A_iP_i]\frac{\partial^2 y}{\partial z^2}-[\gamma_s(A_o-A_i)-A_o\gamma_o + A_i\gamma_i]\frac{\partial y}{\partial z} + m\frac{\partial^2 y}{\partial t^2} + H\frac{\partial^3 y}{\partial z^3} = f'_{ys} \tag{1}$$

$$\frac{\partial^2}{\partial z^2}\left(EI\frac{\partial^2 x}{\partial z^2}\right)-[T(z)-S\cos\omega t + A_oP_o-A_iP_i]\frac{\partial^2 x}{\partial z^2}-[\gamma_s(A_o-A_i)-A_o\gamma_o + A_i\gamma_i]\frac{\partial x}{\partial z} + m\frac{\partial^2 x}{\partial t^2} + H\frac{\partial^3 x}{\partial z^3} = f'_{xs} \tag{2}$$

where EI is flexural rigidity; A_o and A_i are outer and inner cross-sectional areas; P_o and P_i are outer and inner pressures; γ_s, γ_o and γ_i are respectively specific weights of the member, outer fluid and inner fluid; f_{xs} and f_{ys} are hydrodynamic forces in x and y directions; $T(z)$ is axial force; S is the amplitudes of time-varying axial force; m is mass per unit length of the member; H is a torsional component of an external moment; ω is an excitation frequency.

Eqs. (1) and (2) can be reduced to ordinary non-linear differential equations by

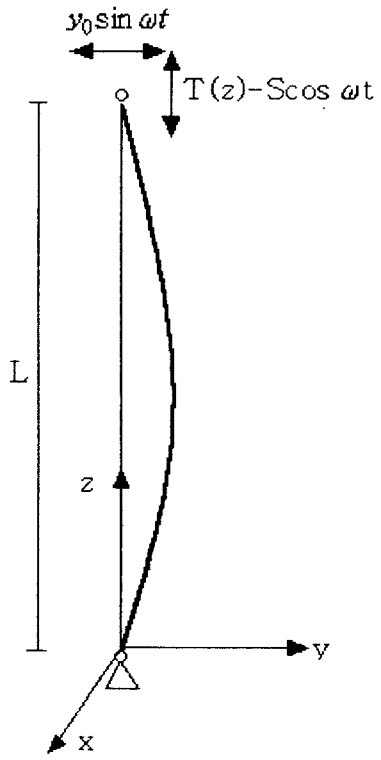

Fig. 2. Model structure configuration and notation.

using separation of variables. In the following, some mathematical rearrangements are made only for Eq. (1) for convenience and a torsional effect is neglected. An approximate solution to Eq. (1) can be written in the form,

$$y(z,t) = -y_0 \sin \omega t \frac{z}{L} + \sum_{n=1}^{\infty} f_n(t) \sin \frac{n\pi z}{L} y(z,t) \tag{3}$$

where L is the model length, $f_n(t)$ is an unknown function of time and y_0 is the amplitude of a surge motion.

Substituting Eq. (3) to Eq. (1), introducing non-dimensional parameters and using the Galerkin's method reduces to the following equation (Patel and Park, 1995).

$$\frac{d^2F_m}{d\tau^2} + (\alpha - \beta\cos\tau)F_m + c_1 \int_0^1 |Q|Q \sin m\pi Z dZ = (-1)^m \frac{2Y_0}{m\pi} \sin\tau \tag{4}$$

where,

$$F_m = \frac{f_m}{d},\ \tau = \omega t,\ \alpha = \left(\frac{\omega_m}{\omega}\right)^2,\ \beta = \frac{S}{EI(m\pi/L)^2 + T_0}\left(\frac{\omega_m}{\omega}\right)^2,$$

$$Q = -Y_0 Z\cos\tau + \sum_{n=1}^{\infty}\left(\sin n\pi Z \frac{dF_n}{d\tau}\right) \omega_m^2 = \frac{EI}{M}\left(\frac{m\pi}{L}\right)^4 + \frac{T_0}{M}\left(\frac{m\pi}{L}\right)^2, \tag{5}$$

$$c_1 = \frac{S}{M}\left(\frac{m\pi}{L}\right)^2,\ Y_0 = \frac{y_0}{d_0},\ Z = \frac{z}{L}$$

where f_m is the amplitude of mth order lateral motions, d_0 is the outer diameter and ω_m is the natural frequency of the mth order of the structure. In the derivation above, the use of the orthogonal property, $\int_0^L \sin(m\pi z/L)\sin(n\pi z/L) = 0$ for $m \neq n$, is made and $T(z)$ is assumed to be T_0.

Eq. (4) is the case for a combined excitation. When only forcing excitation is considered, i.e. when time varying axial force is neglected, Eq. (4) becomes a forced vibration equation.

$$\frac{d^2F_m}{d\tau^2} + \alpha F_m + c_1 \int_0^1 |Q|Q \sin m\pi Z dZ = (-1)^m \frac{2Y_0}{m\pi} \sin\tau. \tag{6}$$

The solution of Eq. (6) can be easily obtained. A similar approach was made by Kirk et al. (1979).

On the other hand, when only the parametric excitation of heaving effect is considered, Eq. (4) takes the following form that is one of the Mathieu equations.

$$\frac{d^2F_m}{d\tau^2} + (\alpha - \beta\cos\tau)F_m + c_1\int_0^1 |R|R\sin m\pi Z dZ = 0 \tag{7}$$

where

$$R = \sum_{n=1}^{\infty}\left(\sin n\pi Z \frac{dF_n}{d\tau}\right).$$

When fluid damping is neglected, the third term in Eq. (7) becomes zero and Eq. (7) becomes a standard Mathieu equation. According to the values of α and β, the solutions of the standard Mathieu equation becomes either stable or unstable (see Fig. 3). If the non-linear fluid damping term is included and linearized, the tips of the unstable zones move upward and become narrower than the case of non-damping. If a quadratic non-linear damping is considered, even the unstable solutions are limited and the maximum values exist in the middle of each instability regions. The β/α is referred as the strength of parametric excitation.

In the previous work (Patel and Park, 1995), the response characteristics of forcing, parametric and combined excitations are semi-analytically obtained (see Fig. 4).

3. Finite element method

An analytical approximate method has some limitations in solving the dynamic characteristics of real complex slender marine structures under combined excitations. Thus a numerical method of FEM is employed here to cope with such problems.

A two-noded beam element using linear displacement functions for axial and torsional effects and cubic functions for bending is used. A 3-D continuum mechanics approach is applied to derive the 12 degrees of freedom (three translations and three rotations per a node).

Based on Eq. (1) and Eq. (2), the equation of motion of a many degrees of freedom system can be derived and written in the following matrix form (Craig, 1981):

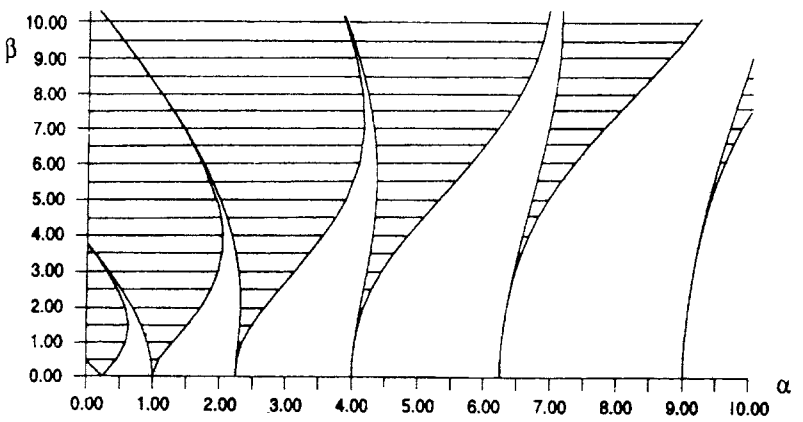

Fig. 3. Mathieu stability chart (shaded areas are unstable).

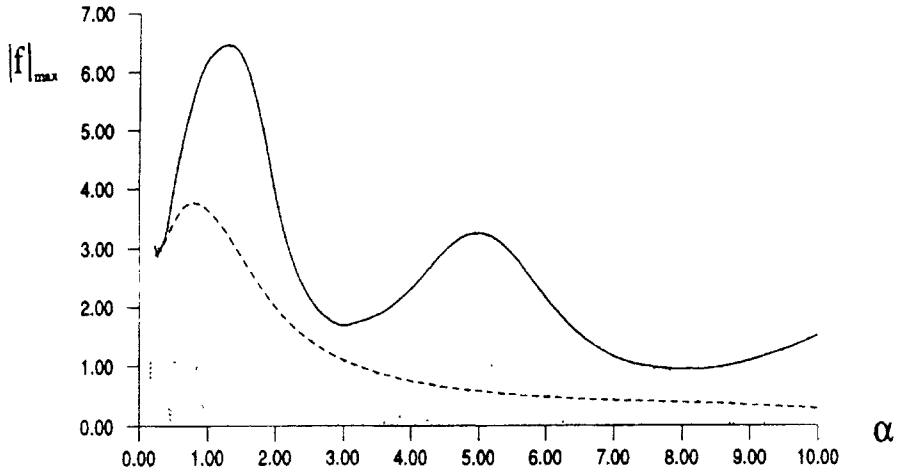

Fig. 4. Comparison between maximum response curves of combined (– –), forcing (—) and parametric (.....) excitations (Patel and Park, 1995).

$$MD + CD + KD = F \tag{8}$$

where D is the matrix of a nodal displacement, and M, C and K are the matrices of structural mass, structural damping and the stiffness respectively. The superscript dot indicates a derivative with respective time t. In the formulation of a beam element mass matrix, lumped mass or consistent mass approach can be used. Lumped mass formulation is chosen in this analysis and all rotational degrees of freedom can be substructured out. The structural damping matrix may be explicitly defined as follows;

$$C = \alpha_0 M + \alpha_1 S. \tag{9}$$

For Rayleigh damping, the coefficients in Eq. (9) can be obtained from the following equation.

$$\alpha_0 = \frac{2(\xi_1\omega_1 - \xi_2\omega_2)}{\frac{\omega_2}{\omega_1} - \frac{\omega_1}{\omega_2}} \tag{10}$$

and

$$\alpha_1 = \frac{2(\xi_2\omega_1 - \xi_1\omega_2)}{\frac{\omega_2}{\omega_1} - \frac{\omega_1}{\omega_2}}$$

where ξ_1 and ξ_2 are respectively damping ratio of first and second natural modes. A damping ratio of 5% in the first two modes has been chosen in this work.

The total stiffness matrix K for an element is derived as the sum of the standard elastic stiffness matrix K_E and a geometric stiffness K_G, that are respectively a function of deflected element geometry and the axial force on the element. Thus,

$$K = K_E + K_G. \tag{11}$$

The stiffness matrix K should be redefined as the function of coordinate and time so as to represent structural properties such as time varying tension given in the following;

$$T_{\text{total}}(z,t) = T(z) - S\cos\omega t \tag{12}$$

where $T_{\text{total}}(z,t)$ is the total time-varying axial force, $T(z)$ is static tension, S is the amplitudes of time-varying axial force and ω is the angular frequency of the time-varying axial force (parametric excitation frequency).

In a forcing excitation problem (a forced vibration problem), K is independent of time and needs to be inverted once only. However, in the case of parametric or combined excitation problems, K needs to be calculated in every time step and requires more computation time than forcing excitation problem.

The external force vector F due to a wave force on the element is obtained from Morison's equation.

$$F_{\text{wave}} = \rho_0 V\dot{U} + \rho_0 V(C_M - 1)(\dot{U} - \ddot{D}) + B|U - \dot{D}|(U - \dot{D}) \tag{13}$$

where V is the vector of elemental volumes, β is the matrix of hydrodynamic drag coefficient, C_M is added inertia coefficient and U, $\dot{U}$ are the wave particle velocity and acceleration in the horizontal direction. The hydrodynamic drag sub-matrix for a fully submerged element is

$$\begin{bmatrix} 0.25\rho_0 C_D L_e d_o & 0 \\ 0 & 0.25\rho_0 C_D L_e d_o \end{bmatrix} \tag{14}$$

where C_D is a drag coefficient and L_e is the element length.

Substituting Eq. (13) into Eq. (8), replacing $[M + \rho_0(C_M - 1)V]$ by M_T and $\rho_0 C_M V$ by M_H, and rearranging gives

$$M_T\ddot{D} + C\dot{D} + K = M_H\dot{U} + B|U - \dot{D}|(U - \dot{D}) \tag{15}$$

where M_T is total structural plus hydrodynamic added mass matrix and M_H is hydrodynamic mass matrix.

The basic method of analysis here involves integrating Eq. (15) through discrete steps in time and accounting the nonlinear drag loading. The Newmark time integration scheme that is known as unconditionally stable, is adopted here. A Fortran program is coded in order to calculate Eq. (15). The program algorithm is based on a riser program (Patel et al., 1984) and expanded from 2-D to 3-D in space.

4. Results and discussion

Some case studies are carried out to analyze the response characteristics of forcing, parametric and combined excitations by using the program. Input data for case study are given in Table 1 that is similar to a TLP tether. Seven different model lengths are chosen but other parameters such as pretension, structure diameter etc. are taken to be identical to each other for the convenience of comparison. It is tended to

Table 1
Input data of a tether model for case studies

Young's modulus (N/m^2)	2.1×10^{11}
Drag coefficient, C_D	0.7
Added mass coefficient, C_M	1.0
Outer diameter (m)	0.812
Thickness (m)	0.0276
Top tension (N)	13×10^6
Material density (kg/m^3)	7850
Vessel surge amplitude (m)	3.0

examine the relative importance of each excitation according to α values, i.e. instability regions. By using the definitions of α and ω_m in Eq. (5) and Fig. 3, the relation between model length, instability region number, fundamental period and α value can be obtained as shown in Table 2. The amplitude of the surge motion, y_0 is assumed to be 3.0m. The strength of parametric excitation, β/α is set to be 1.0.

Although slender marine structures are mostly, in reality, subjected to combined parametric and forcing excitations, the two excitations have been separately considered in most research works. Therefore, comparisons between forcing, parametric and combined excitations are made here to investigate the significance of the combined excitation.

Fig. 5 shows the results of response magnitudes at mid-point of the tether model for forcing, parametric and combined excitations. The results are obtained for four different model lengths, that is, different α values or different instability regions.

Fig. 5(a) is the case of 1365.5m tether length with dynamic condition corresponding to the middle of the first instability region of Mathieu instability chart in Fig. 3. The response amplitudes of the combined excitation are nearly identical to that of forcing excitation. It can be seen that in this first instability region, there is no recognizable interaction between forcing and parametric excitation. Meanwhile, the response periods of the forcing and parametric excitations are respectively identical and double to the excitation period. This is an expected characteristic of forcing and parametric excitations.

Table 2
Relations of α value, instability region number, fundamental natural period and model length

Tether length (m)	Fundamental natural period (s)	α	Instability region
1365.5	30	0.25	Mid first
760.5	15	1.0	Near second
675.0	13.2	1.3	Mid second
525.0	10.0	2.25	Near third
475.0	8.9	2.8	Mid third
400.0	7.5	4.0	Near fourth
360.0	6.7	5.0	Mid fourth

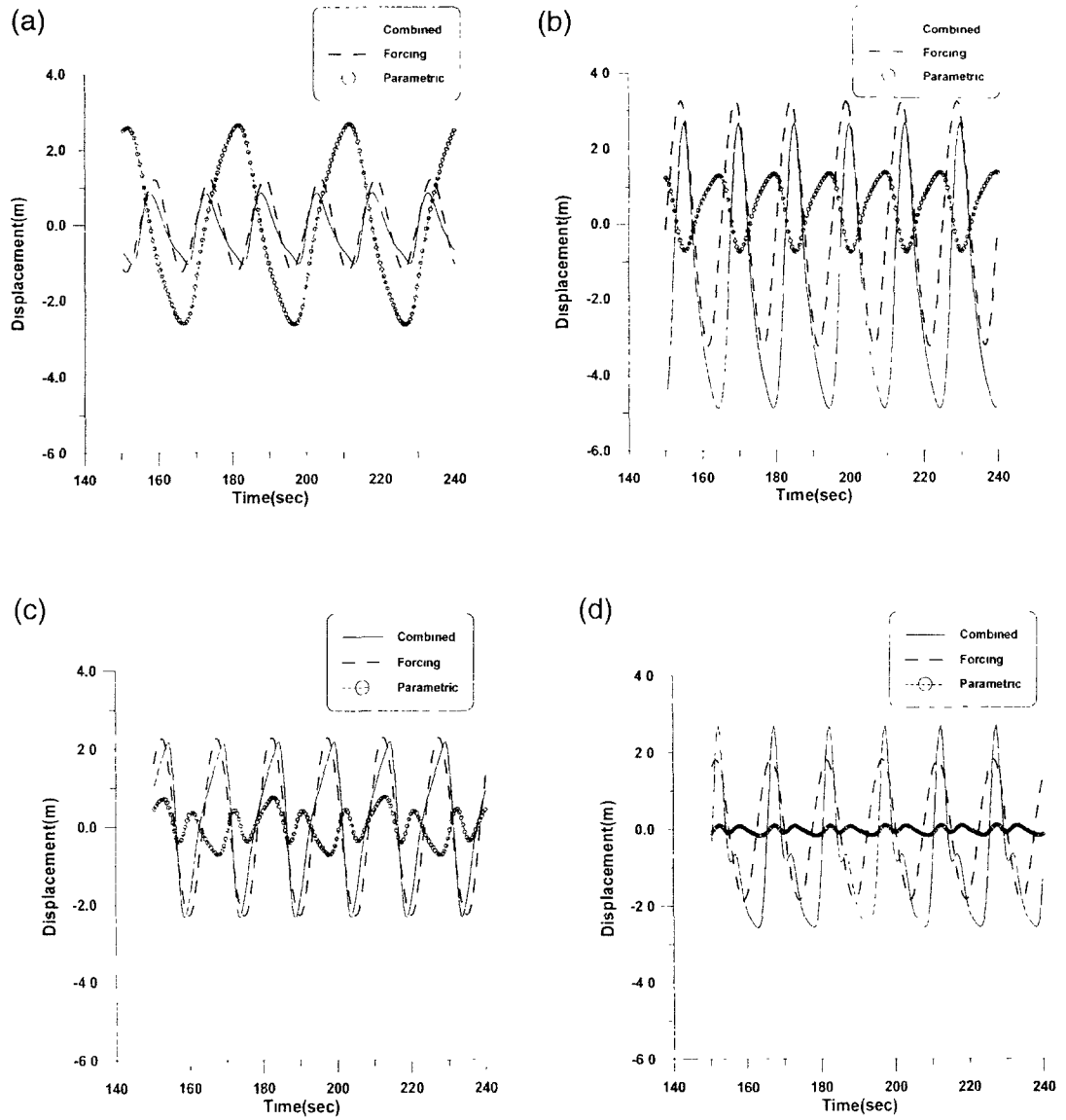

Fig. 5. Comparison of response displacements between combined, forcing and parametric excitations in the middle of each instability region. (a) Mid first instability region (α=0.25). (b) Mid second instability region (α=1.3). (c) Mid third instability region (α=2.8). (d) Mid fourth instability region (α=5.0).

Fig. 5(b) presents results for the case of 675m model with a dynamic condition falling in the middle of the second instability region. Fig. 5(b) shows that the relative response amplitudes of the three excitations in this region are different from those in the above first instability region. In the second instability region, the response amplitudes of the combined excitation are much larger than those of the forcing excitation. This means that the interaction between forcing and parametric excitations is significant in the second instability region. The response periods of the three excitations are all the same as to the excitation period.

Fig. 5(c) illustrates the result for the case of 475m length of tether model with a dominant dynamic condition corresponding to the middle of the third instability region. The response amplitude of the combined excitation is nearly the same as that

of the forcing excitation. The response period of forcing and combined excitations are the same as the excitation period, 15s. But the response periods of parametric excitation is small compared to the excitation period.

Fig. 5(d) shows the result for the case of 360m tether model with dynamic condition corresponding to the middle of the fourth instability region. The pattern of response amplitude is similar to that of the second instability region in Fig. 5(b), i.e. the response amplitudes of the combined excitation are much larger than those of the forcing or parametric excitation.

In addition to the above case studies, the other three cases of 760.5m (α=1.0), 525m (α=2.25) and 400m (α=0) are examined. These dynamic conditions correspond to those somewhat away from the middle of each instability region. The results are given in Fig. 6 and show that relative importance of combined excitation to forcing excitation in such conditions is not large as that in the middle of each instability regions.

Figs. 5 and 6 give similar results to the semi-analytical result in Fig. 4. In the above numerical calculations given in Figs. 5 and 6, it is assumed that excitations come from only surge and heave motions of a surface platform and excitation periods are set to be the first natural period of each tether model in order to compare with semi-analytical results (Patel and Park, 1995). In such a case, the maximum response amplitude occurs at the mid-point of the tether model.

In addition to that, another case study is carried out by considering wave and current effects and using slightly different input data. The input data for the numerical calculations is given in Table 3. The current and wave wards are set to be the negative y-axis and the pretension is greatly reduced that is similar to a riser tension case. The response configurations of the example structure are obtained at the maximum and minimum surge position from z-axis. The results are shown in Fig. 7 and compared between the combined excitation and the forcing excitation. The lateral displacement of the combined excitation is slightly larger than that of the forcing excitation and the difference between two excitations is larger in the mid upper part of the model than the lower part.

These results represent that the response magnitude of the combined excitation is different from that of forcing excitation and thus the combined excitation that is more realistic than forcing excitation needs to be considered for the accurate dynamic analysis of slender marine structures subjected to a surface vessel motion.

5. Conclusions

In this paper, a 3-D numerical analysis using FEM is carried out for the dynamic response of a long slender marine structure under combined forcing and parametric excitations. The relative response amplitudes of combined excitation to conventional forcing excitation were examined by carrying out some case studies for TLP tether and riser type structures with both ends being simply supported. The response pattern of combined excitations is quite different from that of a forcing excitation (a forced vibration problem). The response amplitudes of combined excitation are much greater

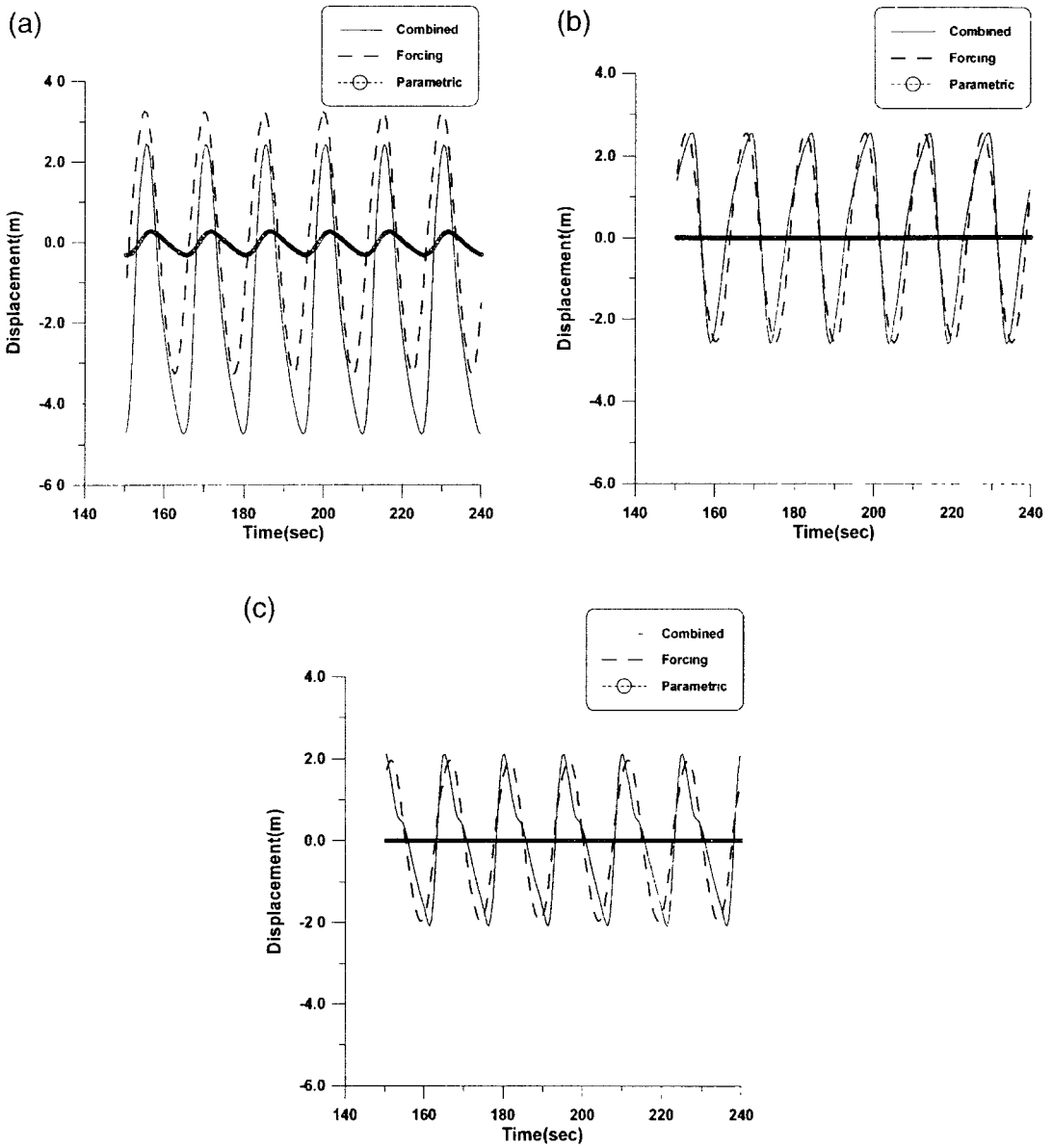

Fig. 6. Comparison of response displacements for different excitations in the near of each instability region. (a) Near second instability region (α=1.0). (b) Near third instability region (α=2.25). (c) Near fourth instability region (α=4.0).

than those of forcing excitation in even numbers of the instability regions of the Mathieu stability chart and are nearly same in other instability regions. The results of this study demonstrate that combined excitation needs to be considered for the exact analysis of long slender marine structures subjected to surface platform motions.

Acknowledgements

Part of this work was completed during a visit by the first author to the Research Institute for Applied Mechanics of Kyushu University. He is very grateful for the

Table 3
Input data for a case study with current and wave effects

Young's modulus (N/m^2)	2.1×10^{11}
Drag coefficient, C_D	0.7
Added mass coefficient, C_M	1.0
Outer diameter (m)	0.812
Thickness (m)	0.0276
Model length (m)	900
Top tension (N)	5.5×10^2
Material density (kg/m^2)	7850
Vessel surge amplitude (m)	3.0
Vessel surge phase angle (°)	15
Wave period (s)	10
Wave height (m)	20
Current velocity (m/s)	Surface:1.0
	Bottom:0

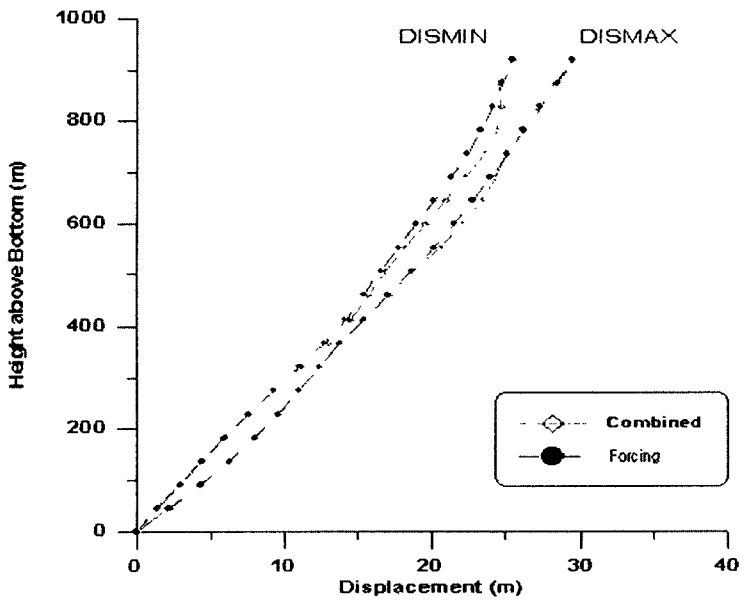

Fig. 7. Comparison of lateral displacements between combined and forcing excitations with wave and current effects.

support provided by the Institute, Korea Science and Engineering Foundation, and Japan Society for the Promotion of Science.

References

Craig, R.R. Jr., 1981. Structural Dynamics. Wiley, New York.

Dareing, D.W., Huang, T.M., 1979. Marine riser vibration response by modal analysis. Journal of Energy Resource Technology, ASME 101, 159–166.

Haquang, N., Mook, D.T., 1987. Nonlinear structural vibrations under combined parametric and external excitations, Journal of Sound and Vibration, 118, 179–181.

Hsu, C.S., 1975. The response of a parametrically excited hanging string in fluid. Journal of Sound and Vibration 39, 305–316.

Kim, Y.C., Triantafyllou, M.M., 1984. The nonlinear dynamics of long slender cylinders. Journal of Energy Resource Technology, ASME 106, 250–256.

Kirk, C.L., Etok, E.U., Cooper, M.T., 1979. Dynamic and static analysis of a riser. Applied Ocean Research, 1, 125–134.

Kokarakis, J.E., Bernitsas, M.M., 1987. Nonlinear three-dimensional dynamic analysis of marine risers. Journal of Energy Resources Technology 109, 105–111.

Moe, G., Leach, C., Erb, P., 1987. Parametric instabilities of disconnected risers. In: Proceedings of the Offshore Mechanics and Arctic Engineering Conference, ASME, Houston, TX, (Vol. 1)., pp. 135–139.

Ohkusu, M., 1990. Study of behaviors of a long and flexible pipe in the water. Journal of the Society of Naval Architects of Japan 167, 137–145.

Patel, M.H., Park, H.I., 1991. Dynamics of TLP tethers at low tension: part 1—Mathieu stability at the large parameters. Marine Structures 4, 257–273.

Patel, M.H., Park, H.I., 1995. Combined axial and lateral responses of tensioned buoyant platform tethers. Engineering Structures 17, 687–695.

Patel, M.H., Sarohia, S., Ng, K.F., 1984. Finite-element analysis of the marine riser. Engineering Structures 6, 175–184.

Patel, M.H., Witz, J.A., 1991. Compliant Offshore Structures. Butterworth Heinemann, Oxford.

Ryu, C.S., Isaacson, M., 1998. Dynamic response analysis of slender maritime structure under vessel motion and regular waves. Journal of Korean Society of Coastal and Ocean Engineering 10 (2), 64–72.

Strickland, G.E., Mason, A.B., 1981. Parametric response of TLP tendons: theoretical and numerical analysis. In: Proceedings of the Offshore Technology Conference, Houston, TX, (Vol. 3)., pp. 45–54.

Thampi, S.K., Niedzwecki, J.M., 1992. Parametric and external excitation of marine risers. Journal of Engineering Mechanics 118 (5), 943–960.